

# Tailoring the reactivity of bimetallic overlayer and surface alloy systems

Axel Groß

*Institut für Theoretische Chemie, Universität Ulm, Albert-Einstein-Allee 11, 89069 Ulm/Germany*

Changing the composition and structure of a bimetallic surface system modifies its electronic properties and thus its catalytic activity. Based on density functional theory calculations, we will discuss the electronic factors underlying the modified properties of bimetallic surfaces such as overlayer systems and in particular surface alloys. It will be demonstrated that by mixing two metals a new metallic compound can result whose properties are not intermediate but beyond those of both constituents so that for example by adding a relatively inert metal a more reactive surface can result. Besides the reactivity also the stability of the bimetallic systems will be briefly discussed.

## 1. INTRODUCTION

Many chemical reactions are significantly accelerated when they occur in the presence of a solid surface, in particular metallic surfaces. This is the basis of heterogeneous catalysis which is of tremendous technological importance. However, catalytic reactions are also interesting from a fundamental point of view. A true understanding of the underlying electronic factors governing of chemical activity can ultimately even lead to the design of novel catalysts [1]. Catalytically active metals are mainly late transition metals such as platinum or palladium. By mixing different metals, alloys result which may have improved catalytic activity and selectivity. Another important aspect is to identify catalysts based on less expensive and more available metals [2]. In this context, in particular bimetallic catalysts have been studied intensively, both at the solid-vacuum as well as the solid-liquid interface [3–11].

The activity of bimetallic catalysts is often discussed using the concepts of the *ensemble* and the *ligand* effect [3, 12]. The term *ensemble* effect refers to those reactions where a certain number of active sites is required for the reaction to occur so that by blocking a large ensemble of active sites this reaction can be suppressed. For example, the selectivity towards reactions that only need a small ensemble of active sites can thus be increased. The catalytic activity of a bimetallic system is also modified by the direct chemical interactions between the components which influence their electronic structure and thus their catalytic activity; this is called the *ligand effect*. In addition to this pure electronic effect, the modifications of the interatomic distances in a bimetallic system can also have a significant influence on its electronic structure and thus on its catalytic activity. This *geometric effect* should also be taken into account together with the ensemble and ligand effects when the reactivity of bimetallic systems is discussed. Experimentally, it is often not easy to disentangle all these effects. In this review, I will show that first-principles total energy studies based on periodic density functional theory (DFT) calculations are well capable of discriminating between them by selecting appropriate systems which are not necessarily realistic but are governed by one particular mechanism.

In order to discuss the trends found in the catalytic activity of bimetallic systems as a function of modified interatomic distances and/or the chemical interaction, the *d*-band model [13, 14] has been quite successful: for example, tensile strain or the interaction with an inert metal species leads to a narrowing of the metal *d*-band due to the reduced overlap of the wave functions. If the *d*-band is more than half-filled, i.e., if the metal is a late transition metal, then the band narrowing leads to an increase in its fraction that lies below the Fermi energy and consequently to a higher population of the *d*-band. Because of charge conservation, however, the *d*-band moves up in order to preserve its degree of *d*-band filling [15]. And according to the *d*-band model, there is a linear relationship between the *d*-band center shift  $\delta\epsilon_d$  and the change in the chemisorption strength  $\Delta E_d$  [16, 17],

$$\delta E_d = -\frac{V^2}{|\epsilon_d - \epsilon_a|^2} \delta\epsilon_d, \quad (1)$$

where  $\epsilon_a$  is an electronic adsorbate level and  $V$  is a coupling matrix element that is assumed to be constant for similar situations. This means that the upshift of the *d*-band upon lattice expansion or reduced interaction in late *d*-band metals causes a stronger interaction with adsorbates. It is important to realize that the higher binding to lower coordinated sites at nanostructured surfaces can be explained by a similar reasoning [14, 18]: A lower coordination, i.e., a smaller number of nearest neighbors also leads to a band narrowing and a subsequent upshift of the *d*-band center.

In a previous work, our studies of bimetallic overlayer systems were already reviewed [6] showing that the *d*-band model can indeed be applied successfully to explain the chemical trends found in these overlayer systems. I will briefly summarize these findings and mainly concentrate on surface alloys in this review. I will in particular emphasize that the mixing of two metals can lead to a compound whose properties are beyond those of the single constituents. Furthermore, we will briefly address the issue of the stability of bimetallic systems which is important for the use of bimetallic systems in real catalysts.

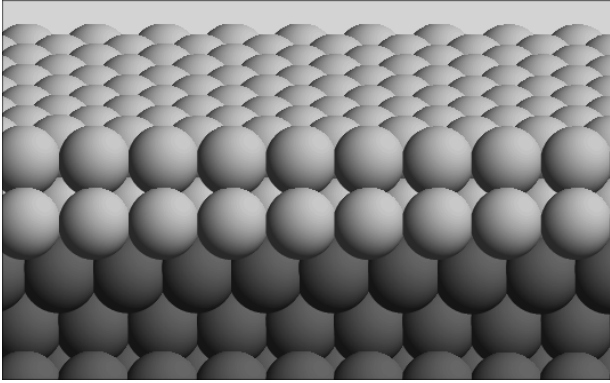


FIG. 1: Illustration of the structure of a bimetallic overlayer system.

## 2. ADSORPTION ON BIMETALLIC OVERLAYER SYSTEMS

In this section, we will discuss the reactivity of bimetallic overlayer systems. First a note of caution should be made as far as the definition of reactivity is concerned. Here we will mainly identify reactivity with the interaction of the surfaces with adsorbates. However, high catalytic activity usually is the consequence of a compromise. On the one hand, the interaction between the catalyst and the reactants should be sufficiently strong in order to lead to, e.g., lower dissociation barriers than in the gas phase. On the other hand, this interaction should be weak enough so that the products can desorb again. Still, the interaction strength of molecules with surfaces is often closely correlated with the reactivity for a large class of catalytic reactions, for example via a Brønsted-Evans-Polanyi-type relation [19].

A typical overlayer system is illustrated in Fig. 1. I will only consider pseudomorphic layers here which means that the overlayer atoms will have the same lateral lattice spacing as the substrate. This induces strain in the overlayer when there is a lattice mismatch in the lattice constants of substrate and overlayer. It is now well-established that strain can significantly modify adsorption energies and reaction barriers on surfaces [20–24]. In addition, there is the direct electronic interaction between overlayer and substrate.

The first system I will address is the PtRu system. This system is of strong current interest in the context of CO tolerant fuel cell catalysts. CO binds so strongly to many catalysts that they become poisoned because all catalytic active sites are blocked by CO. Experimentally it has been confirmed that the addition of Ru to Pt leads to an increased CO tolerance [9, 25, 26] which means that this bimetallic catalyst is not that easily poisoned by CO.

In order to shed light on the microscopic mechanism of this increased CO tolerance of the PtRu system, a combined experimental and theoretical study of the adsorption of CO on Pt layers on Ru(0001) was performed [27].

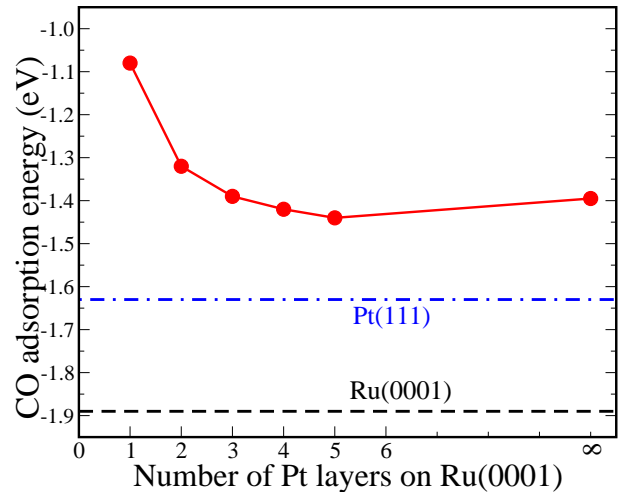


FIG. 2: Calculated CO adsorption energy on  $Pt_n/Ru(0001)$  overlayers at the top site as a function of the number  $n$  of overlayers (after [27]). The dashed and the dash-dotted lines denote the corresponding result for pure Ru(0001) and pure Pt(111), respectively. The CO adsorption energy for an infinite number of Pt layers on Ru(0001) correspond to a Pt slab calculation with the lateral lattice constant of Ru.

The lattice constant of Pt is 2.5% larger than the one of Ru; still Pt grows pseudomorphically on Ru(0001) up to at least four monolayers [27, 28] which allows a close comparison between experimental and theoretical results. Experimentally, it was found that the desorption temperature of CO on Pt/Ru overlayers rises with increasing number of Pt monolayers indicating a stronger binding for a larger number of Pt layers. Still, the CO desorption temperatures are well below the corresponding temperatures on pure Pt(111) as well as on Ru(0001) [27].

Calculated DFT adsorption energies of CO on Pt/Ru(0001) as a function of the number of Pt overlayers are shown in Fig. 2. The DFT calculations were performed using the generalized gradient approximation (GGA) to describe the exchange-correlation effects [29]. The adsorption energy of the CO molecule was calculated according to

$$E_{\text{ads}} = E_{\text{surf+CO}} - (E_{\text{surf}} + E_{\text{CO}}) \quad (2)$$

where  $E_{\text{surf+CO}}$  is the total energy of the bimetallic substrate with the adsorbed CO while  $E_{\text{surf}}$  and  $E_{\text{CO}}$  are the energies of the corresponding clean bimetallic system and the free CO molecule, respectively. It should be noted that the adsorption energy becomes negative for stable adsorption. With the term “binding energy” I will refer to the absolute value of the adsorption energy. The CO adsorption energy plotted in Fig. 2 for an infinite ( $\infty$ ) number of Pt layers was obtained for a Pt(111) substrate with the lateral lattice constant of Ru. In addition, the CO adsorption energies on pure Pt(111) and Ru(0001) are plotted.

As far as the adsorption of CO on Pt(111) is concerned, DFT calculations yield the wrong adsorption

site: whereas experiments find the top site to be the most favorable adsorption site for the CO molecule on the Pt(111) surface, periodic DFT calculations using local or semi-local functionals predict the fcc hollow site to be more stable [30]. There is evidence that this so-called CO/Pt puzzle is caused by the overestimation of the back-donation into the  $2\pi^*$  orbital of CO which is mainly due to the fact that the HOMO-LUMO gap is too small in most of the semi-local DFT exchange-correlation functionals [31]. Using the GGA+ $U$  method to enlarge the HOMO-LUMO gap leads to a correct site assignment [31]. However, the DFT studies presented here are concerned with chemical trends as a function of the bimetallic atomic configuration. These should be reliably reproduced by first-principles calculations regardless of the correct site preference. Hence only the top site was considered in the study of the CO adsorption on Pt/Ru overlayer systems [27, 32].

Inspecting Fig. 2, first of all it is obvious that the CO binding energies on all considered PtRu systems are smaller than the CO binding energies on Pt(111) and Ru(0001). This is an example for the case mentioned in the introduction: the CO binding energies on the bimetallic system are below those on both pure components, i.e., the bimetallic compound shows properties that are beyond those of the single constituents. Similar results have also been found for the CO adsorption at the top sites of PtRu alloy surfaces [33].

This reduced binding of CO to the Pt/Ru overlayer systems is due to a combination of geometric and direct electronic (ligand) effects, as a careful analysis of the DFT calculations reveals. The comparison of the results for the CO adsorption on relaxed Pt(111) and Pt(111) with the lateral lattice constant of Ru demonstrates the effect of the lattice strain on the CO binding. Here we have the opposite scenario as outlined in the introduction: the Pt layer on Ru(0001) is compressed by 2.5% which leads to a broadening of its local  $d$ -band and consequently to a downshift of its  $d$ -band center, as confirmed in the DFT calculations [27, 34]. This explains a reduction in the CO binding by 0.2 eV upon the compression of the Pt layer.

There is a further weakening of the binding of CO to the Pt/Ru(0001) overlayer system when the number of Pt overlayers is reduced. It is important to note that Ru with its only slightly more than half-filled  $d$ -band is rather reactive. It has a large cohesive energy and is also strongly interacting with the Pt overlayer which is associated with a strong downshift of the  $d$ -band center of the Pt atoms. Using bond order concepts, the strongly reduced binding of CO to one Pt overlayer on Ru(0001) can be explained by the strong direct Pt-Ru interaction which makes Pt interact less strongly with adsorbates. Figure 2 demonstrates that the influence of the direct Pt-Ru interaction is only operative for CO binding to the first two Pt overlayers, for more than two overlayers its effect is only minor.

The same trends as just discussed have also been found

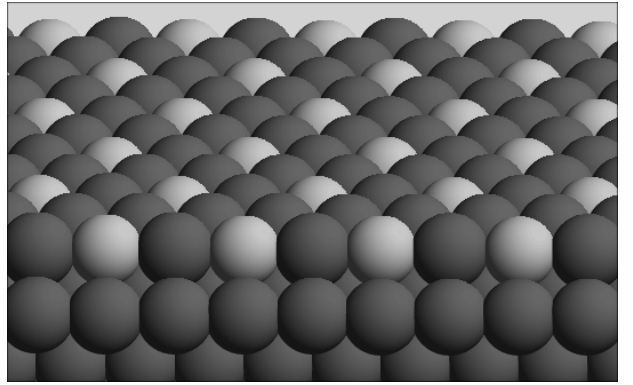


FIG. 3: Illustration of the structure of a bimetallic surface alloy on a (111) substrate restricted to the first surface layer.

on PtRu alloys [33] and also in the adsorption of atomic and molecular oxygen on Pt/Ru overlayers [34]. Hence the findings discussed in this section can be summarized in the hypothesis that depositing a less reactive metal (Pt) on a more reactive metal (Ru) makes the overlayer even less reactive.

### 3. BIMETALLIC SURFACE ALLOYS

Bimetallic overlayer systems are very interesting from a fundamental point of view because they allow a discrimination of direct electronic and geometric strain effects, as just demonstrated for the Pt/Ru system. However, usually these overlayer systems are often not thermodynamically stable against either segregation or intermixing of the two compounds. Even if some metals are immiscible in the bulk they might still be able to form alloys at the surface. These *surface alloys* correspond to ultrathin alloy films on top of some substrate. Such a situation is illustrated in Fig. 3 where a ordered monolayer surface alloy with a  $(2 \times 2)$  structure on a (111) substrate is shown. If the two components of a bimetallic system are also miscible in the bulk, then a alloy restricted to the surface region can still be prepared but will correspond to a metastable structure whose transformation is kinetically hindered.

Experimentally, the adsorption of CO on ultrathin CuPd alloys deposited on Ru(0001) was studied [36] using temperature-programmed desorption (TPD). As far as pure pseudomorphic Pd and Cu monolayers on Ru(0001) are concerned, the TPD experiments found that the CO binding on Pd/Ru(0001) is weaker and on Cu/Ru(0001) stronger than on the corresponding elemental surfaces. This can be understood taken into account strain effects because Pd is compressed and Cu expanded on Ru(0001). As for the PdCu surface alloys on Ru(0001), the experimentalists speculated that ensemble, ligand and strain effects act in a cooperative, synergetic manner [36]. These experimental findings motivated a theoretical study addressing the interaction of CO with

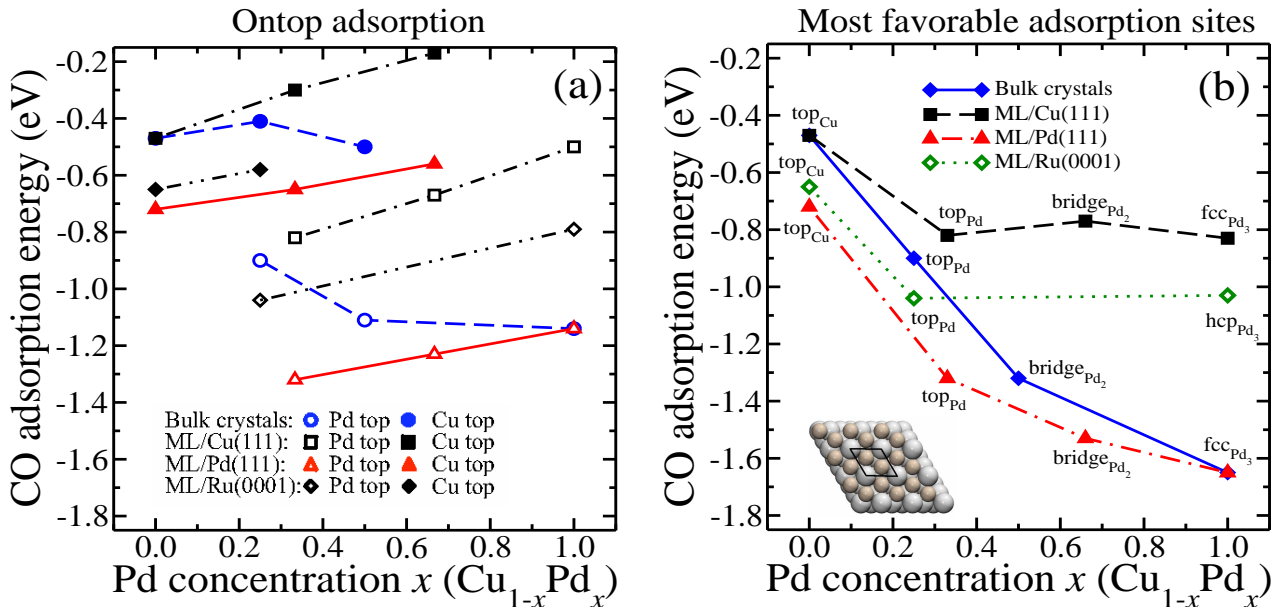


FIG. 4: CO adsorption energies on the top (a) and the most favorable adsorption sites (b) of CuPd monolayer surface alloys on Cu(111) and Pd(111) calculated as a function of the Pd concentration in the surface alloy [35]. The inset shows the structure of the ordered Cu<sub>2</sub>Pd surface alloy.

CuPd surface alloys on Cu(111), Pd(111) and Ru(0001) by means of periodic DFT calculations [35].

The calculated CO adsorption energies at the top and the most favorable adsorption sites of pseudomorphic CuPd monolayer surface alloys on Cu(111), Pd(111) and Ru(0001) are shown in Fig. 4a and Fig. 4b, respectively, as a function of the Pd concentration in the surface alloy. Note that Pd is usually catalytically more active than the noble metal Cu because the Pd  $d$ -band is not completely filled. At the top sites, CO is mainly interacting with the metal atom direct beneath it. Astonishingly, Fig. 4a demonstrates that the adsorption energies of CO on all top sites become less negative, i.e., the binding energies become smaller when the Pd concentration is increased. This means that the *single* Cu and Pd atoms in this surface alloy interact less strongly with CO when the more reactive metal Pd is added. This surprising behavior becomes clear when the size of the Pd and Cu atoms are considered. The  $4d$  metal Pd has a lattice constant that is 8% larger than the one of the  $3d$  metal Cu. Thus increasing the Pd concentration in the surface alloys metal substrate corresponds to replacing smaller Cu atoms by larger Pd atoms. This effectively induces a compressive strain in the surface alloy monolayer, and this compression leads to a reduction in the interaction of the single metal atoms with CO, similar to the case of Pt overlayers on Ru presented in the previous section.

In Fig. 4a, we have considered CO ontop adsorption as a probe of the reactivity of the single metal atoms. However, as far as the adsorption at the energetically most favorable sites on the PdCu surfaces alloys are concerned (Fig. 4b), it is obvious that the CO binding becomes stronger with increasing Pd concentration. On Pd, CO

prefers high-coordinated adsorption site. Consequently, at the ordered surface alloys, the most favorable adsorption sites change from the Pd top site over the Pd bridge site to the three-fold coordinated Pd hollow site with increasing Pd concentration. This means that the binding energies of CO to the CuPd surface alloys exhibits an ensemble effect: it becomes stronger with the availability of higher-coordinated Pd sites in spite of the fact the single Pd atoms interact less strongly with CO for increasing Pd coverages. Hence ensemble and ligand effects show opposite trends as a function of the Pd concentration in CuPd surface alloys.

Next we discuss PtAu bimetallic structures on Au(111). Here again we add the more reactive metal (Pt) to a noble metal (Au), however, now this more reactive metal has a lattice constant that is 5% smaller than the one of the noble metal Au. Both Pt/Au(111) overlayer systems as well as one- and two-layer PtAu surface alloys on Au(111) were considered in DFT calculations [37, 38]. The CO adsorption energies on these different bimetallic systems at the top sites and at the energetically most favorable sites as a function of the Pt concentration given in monolayers (ML) are plotted in Fig. 5. For the relaxed Pt(111) surface, the wrong site assignment is demonstrated in Fig. 5: the three-fold hollow site is predicted to be more stable than the top site, in contrast to the experiment [30], as discussed above. Interestingly, at a Pt slab with the larger lateral lattice constant of Au, denoted by  $\infty$  in Fig. 5, both adsorption sites become practically degenerate. Furthermore, there is a much stronger binding at the expanded Pt(111) surface, as expected from the previous examples.

We will first concentrate on the CO adsorption at the

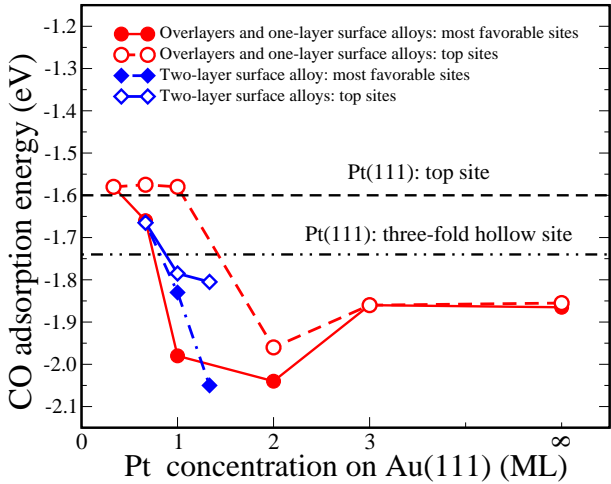


FIG. 5: Calculated CO adsorption energy on bimetallic PtAu/Au(111) surfaces as a function of the Pt concentration measured in monolayers (ML). Circles: CO adsorption on overlayer and one-layer surface alloys; diamonds: CO adsorption on a two-layer surface alloy with a  $\text{Pt}_1\text{Au}_2$  stoichiometry in the second layer. Filled symbols: CO adsorption at the most favorable adsorption sites; open symbols: CO adsorption at top sites. The CO adsorption energy for an infinite concentration of Pt corresponds to a Pt slab calculation with the lateral lattice constant of Au. In addition, the CO adsorption energies at the three-fold hollow and the top site of relaxed Pt(111) are indicated by the horizontal lines (after [37, 38]).

most favorable adsorption sites. For three Pt layers on Au(111), there is almost no direct influence of the underlying Au(111) substrate, indicated by the fact that the CO adsorption energies do not differ from the values of the expanded pure Pt(111) surface. However, reducing the number of Pt layers to two leads to a significantly stronger binding. This can be explained by the weak interaction between Pt and Au: Because the Pt atoms are relatively weakly coupled to Au, they can bind adsorbates more strongly. This is also reflected in the corresponding shift of the local Pt  $d$ -band center [37]. Interestingly enough, for one-layer PtAu surface alloys the CO binding becomes weaker again, however, this trend reversal can not be derived from the position of the  $d$ -band center [37]. A careful analysis reveals that rather a long-range direct repulsion between CO and the Au atoms of the substrate are responsible for this effect [37]. Exactly the same behavior has also been found for the adsorption on Pd/Au overlayer systems [39, 40].

As far as the CO adsorption at the Pt top sites of the one-layer surface alloys is concerned, it is basically independent of the Pt concentration, in contrast to the PdCu surface alloys shown in Fig. 4a. In fact, for the PtAu surface alloys we have two counteracting effects. Adding noble Au atoms to the surface alloy reduces the mutual interaction between the metal atoms in the first layer which makes the Pt atoms more reactive. On the other hand, the addition of the larger Au atoms effec-

tively induces compressive strain in the first layer which makes the Pt atoms less reactive. Obviously, both effects nearly cancel each other leading to CO adsorption energies at the top sites that are practically independent of the composition.

Interestingly, the replacement of an Au atom in the second layer by a Pt atom results in a stronger binding of CO, as the comparison of the one-layer and two-layer surface alloy results in Fig. 5 indicates. Obviously, the additional Pt atom in the second layer reduces the direct second-layer repulsion. Furthermore, an analysis of the electron density revealed that due to the lower symmetry of the two-layer surface alloy compared to the one-layer surface alloy there is a better coupling of the CO  $\sigma$  orbitals with the Pt  $d$  orbitals. Thus the maximum binding energy is obtained for a Pt concentration of 1.33 ML. This is in fact in good agreement with the experiment that found the maximum CO binding at approximately 1.3 ML coverage of Pt [41].

It is important to note that on both the Pt/Au and the Pd/Au overlayer systems and on the PtAu surface alloys with a concentration of more than 1 ML the CO binding is stronger than on the pure metal surfaces. Based on these findings, the following hypothesis can be made: Depositing a more reactive metal on a more inert metal with a larger lattice constant makes it even more reactive. A similar conclusion was also drawn in a combined experimental and theoretical study of the  $\text{NO}_x$  decomposition over silver-rhodium bimetallic surfaces where the addition of the unreactive noble metal enhances the catalytic activity [42].

#### 4. STABILITY OF SURFACE ALLOYS

So far we have determined the interaction of bimetallic overlayer systems and surface alloys with adsorbates for a variety of different given structures. We have identified some of the microscopic mechanisms that lead to an enhanced reactivity of these bimetallic surfaces. However, an industrially used catalyst material often has to sustain rather harsh conditions such as high temperatures and pressures. Hence the stability of bimetallic structures is an important issue in the design of catalyst with improved properties. This is particularly important for bimetallic nanostructures such as deposited metal clusters [18] which might easily show sintering effects at higher temperatures.

An important quantity for the stability of surface alloy is the formation energy which corresponds to the energy gain or cost upon the formation of the bimetallic system from an elemental substrate with the corresponding number of metal atoms exchanged with bulk reservoirs. For the PtAu/Au(111) surface alloys, this formation energy can be evaluated using

$$E_{\text{form}} = E_{\text{Pt}_x\text{Au}_{(1-x)}/\text{Au}(111)} - [E_{\text{Au}(111)} + x(E_{\text{Pt}}^{\text{coh}} - E_{\text{Au}}^{\text{coh}})] \quad (3)$$

Here,  $E_{\text{Pt}_x\text{Au}_{(1-x)}/\text{Au}(111)}$  is the total energy of the

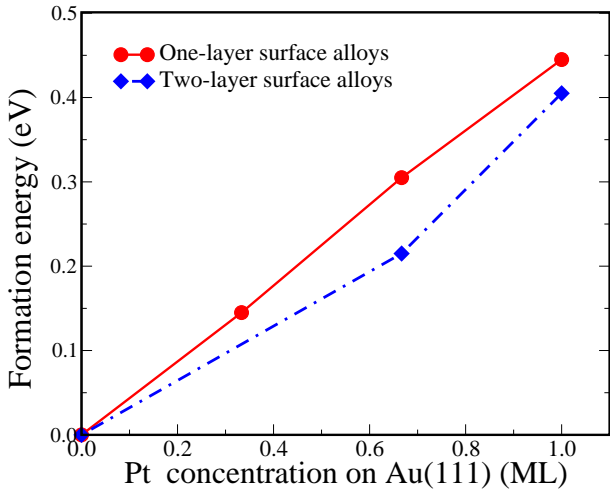


FIG. 6: Surface alloy formation energy  $E_{\text{form}}$  determined according to Eq. (3) for one-layer (circles) and two-layer (diamonds) PtAu surface alloys on Au(111) (after [38]).

$\text{Pt}_x\text{Au}_{(1-x)}/\text{Au}(111)$  electrode,  $E_{\text{Au}(111)}$  is the one of the Au(111) electrode without Pt, and  $E_X^{\text{coh}}$  is the cohesive energy of element X.

The calculated formation energies for one-layer and two-layer PtAu surface alloys on Au(111) are plotted in Fig. 6. It is obvious that all calculated surface alloy formation energies are positive. This indicates that these PtAu surface alloys on Au(111) are not thermodynamically stable so that they can not be used in real catalysts. The systems might not only exhibit segregation of the constituents, but the added metal species might also diffuse into the bulk which is usually the case for atoms that are smaller than the substrate atoms, as for Pt on Au. However, the conversion of the surface alloy is kinetically hindered so that it is still possible to perform surface science experiments with these surface alloys, as demonstrated [41], as long as the temperatures in the experiment are not too high. Furthermore, it is interesting to note that the two-layer surface alloys are more stable than the one-layer surface alloys, most probably because of a better strain relief in the two-layer PtAu surface alloys at the same Pt concentration.

All the bimetallic systems considered so far correspond to ordered structures with rather small surface unit cells because of the computational costs associated with calculating structures with larger unit cells. However, surface alloys are not necessarily ordered, and even if they exhibit a short-range order, there might be no long-range order. In order to address such systems, DFT calculations are too time-consuming. However, it is still possible to address such alloy systems based on first-principles results. The energetics of the alloy system can be expressed using the so-called lattice gas Hamiltonian [43]

$$H(\{\vec{R}\}) = \sum_{\vec{R}_i} E(\vec{R}_i) n_i + \frac{1}{2} \sum_{\vec{R}_i} \sum_{\vec{R}_j} V_2(\vec{R}_i, \vec{R}_j) n_i n_j + \frac{1}{6} \sum_{\vec{R}_i} \sum_{\vec{R}_j} \sum_{\vec{R}_k} V_3(\vec{R}_i, \vec{R}_j, \vec{R}_k) n_i n_j n_k + \dots (4)$$

where  $E(\vec{R}_i)$  is the single-particle energy of a atom at site  $\vec{R}_i$ , and  $V_2$  and  $V_3$  are the two-particle and three-particle interactions, respectively. The occupation numbers  $n_i$  are either 0 or 1 depending on whether the adsorption site in cell  $\vec{R}_i$  is empty or occupied. Note that the same model for the three-dimensional bulk description is known as the *cluster expansion* [44]. Usually only two-particle interactions are included, but for certain problems also so-called *triples* corresponding to three-particle interactions have to be included [45].

The parameters  $E, V_2, V_3, \dots$  appearing in Eq. (4) can either be derived from experiment or from periodic DFT calculations. For PdCu surface alloys, effective pair interaction (EPI) parameters

$$V_{ij} = \frac{1}{2} (V_{ij}^{AA} + V_{ij}^{BB} - 2V_{ij}^{AB}) \quad (5)$$

for  $A = \text{Pd}$  and  $B = \text{Cu}$  were determined from atomic resolution scanning tunneling microscopy (STM) images using Monte Carlo simulations [46]. These parameters describe the energetic difference between like and unlike pairs atoms at sites  $\vec{R}_i$  and  $\vec{R}_j$ . For example,  $V_{ij} < 0$  corresponds to a more attractive interaction between unlike pairs favoring mixing. Using these parameters, the ground state structures and mixing energies at 0 K were determined and compared to mixing energies derived from DFT calculations of different ordered surface alloys, yielding a good agreement.

Figure 7 shows simulated images of  $\text{Cu}_2\text{Pd}$  surface alloys on Ru(0001) at 1 K (a) and 600 K (b) obtained with a Monte Carlo algorithm. At 1 K, a rather well-ordered structure is formed. This is a consequence of effective nearest-neighbor attraction between unlike neighbors, and it is also reflected by a negative mixing or alloy formation energy in both the Monte Carlo based EPI and the DFT calculations.

However, at higher temperatures, as demonstrated in Fig. 7b, there is no short-range order any more. According to a more quantitative analysis, the order-disorder transition occurs at a temperature of about  $T_c = 100 \text{ K}$ . A similar low value of  $T_c$  was also reported for PdAu/Ru(0001) surface alloys [47]. These values are much smaller than the transition temperatures for the corresponding bulk alloys. This can be explained by the lower coordination of the atoms in a surface alloy compared to a bulk alloy which reduces the energy costs associated with a defect in an ordered structure so that the entropic driving force for disordered structure is operative at lower temperatures. This explains why in the experiment no ordered CuPd structures were found. The

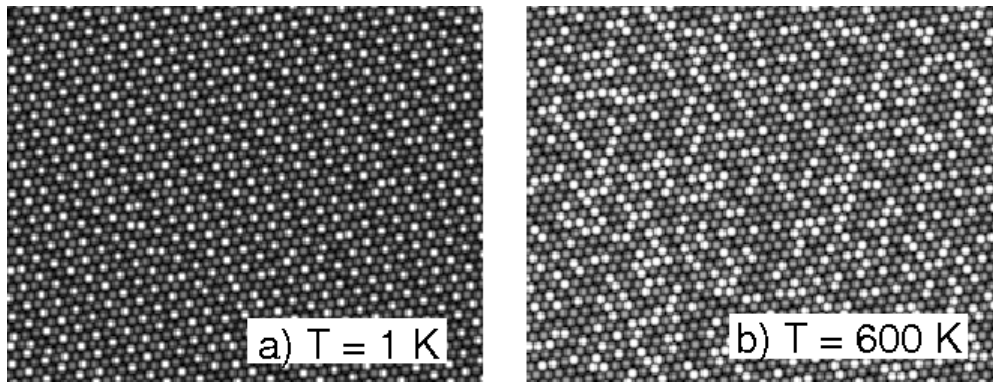


FIG. 7: Structure of simulated PdCu<sub>2</sub> surface alloys on Ru(0001) at 1 K (a) and 600 K (b) (after [46]).

preparation of the surface alloys requires temperatures above 600 K to provide sufficient mobility for diffusion and intermixing within a reasonable period of time, and at these high temperatures, no ordered structures form.

## 5. CONCLUSIONS

In this brief review it was shown that the properties of bimetallic overlayer systems and surface alloys can be distinctly different from those of the single constituents. For example, adding an inert metal can lead to an enhanced catalytic activity. However, in addition to the modified

reactivity of the bimetallic systems also their stability is an important issue which can also be addressed from first principles combined with statistical approaches. The insights gained from theoretical studies might open the way to the rational design of catalysts materials with desired catalytic activity, selectivity, and stability

## Acknowledgments

The studies reported in this review were made possible by grants of the Deutsche Forschungsgemeinschaft and the Alexander von Humboldt Foundation.

- 
- [1] F. Besenbacher, I. Chorkendorff, B. S. Clausen, B. Hammer, A. M. Molenbroek, J. K. Nørskov, and I. Stensgaard, *Science*, **279**, 1913 (1998).
- [2] F. Studt, F. Abild-Pedersen, T. Bligaard, R. Z. Sørensén, C. H. Christensen, and J. K. Nørskov, *Science*, **320**, 1320 (2008).
- [3] J. A. Rodriguez, *Surf. Sci. Rep.*, **24**, 223 (1996).
- [4] J. H. Sinfelt, *Surf. Sci.*, **500**, 923 (2002).
- [5] J. Greeley and M. Mavrikakis, *Nature Materials*, **3**, 810 (2004).
- [6] A. Groß, *Topics Catal.*, **37**, 29 (2006).
- [7] F. Maroun, F. Ozanam, O. M. Magnussen, and R. J. Behm, *Science*, **293**, 1811 (2002).
- [8] J. L. Zhang, M. B. Vukmirovic, K. Sasaki, A. U. Nilekar, M. Mavrikakis, and R. R. Adzic, *J. Am. Chem. Soc.*, **127**, 12480 (2005).
- [9] F. Buatier de Mongeot, M. Scherer, B. Gleich, E. Kopatzki, and R. J. Behm, *Surf. Sci.*, **411**, 249–262 (1998).
- [10] A. Roudgar and A. Groß, *Chem. Phys. Lett.*, **409**, 157 (2005).
- [11] D. M. Kolb, *Surf. Sci.*, **500**, 722 (2002).
- [12] W. H. M. Sachtler, *Faraday Diss.*, **72**, 7 (1981).
- [13] B. Hammer and J. K. Nørskov, *Surf. Sci.*, **343**, 211 (1995).
- [14] A. Groß, *J. Comput. Theor. Nanosci.*, **5**, 894 (2008).
- [15] A. Ruban, B. Hammer, P. Stoltze, H. L. Skriver, and J. K. Nørskov, *J. Mol. Catal. A*, **115**, 421 (1997).
- [16] B. Hammer, O. H. Nielsen, and J. K. Nørskov, *Catal. Lett.*, **46**, 31 (1997).
- [17] V. Pallassana, M. Neurock, L. B. Hansen, B. Hammer, and J. K. Nørskov, *Phys. Rev. B*, **60**, 6146 (1999).
- [18] A. Roudgar and A. Groß, *Surf. Sci.*, **559**, L180 (2004).
- [19] J. K. Nørskov, T. Bligaard, A. Logadottir, S. Bahn, L. B. Hansen, M. Bollinger, H. Bengaard, B. Hammer, Z. Sljivančanin, M. Mavrikakis, Y. Xu, S. Dahl, and C. J. H. Jacobsen, *J. Catal.*, **209**, 275 (2002).
- [20] M. Gsell, P. Jakob, and D. Menzel, *Science*, **280**, 717 (1998).
- [21] M. Mavrikakis, B. Hammer, and J. K. Nørskov, *Phys. Rev. Lett.*, **81**, 2819 (1998).
- [22] J. Wintterlin, T. Zambelli, J. Trost, J. Greeley, and M. Mavrikakis, *Angew. Chem. Int. Ed.*, **42**, 2850 (2003).
- [23] S. Sakong and A. Groß, *Surf. Sci.*, **525**, 107 (2003).
- [24] S. Sakong and A. Groß, *J. Catal.*, **231**, 420 (2005).
- [25] H. Massong, H. Wang, G. Samjeské, and H. Baltruschat, *Electrochim. Acta*, **46**, 701 (2000).
- [26] H. Hoster, B. Richter, and R. J. Behm, *J. Phys. Chem. B*, **108**, 14780 (2004).
- [27] A. Schlapka, M. Lischka, A. Groß, U. Käsberger, and P. Jakob, *Phys. Rev. Lett.*, **91**, 016101 (2003).
- [28] P. Jakob and A. Schlapka, *Surf. Sci.*, **601**, 3556 (2007).
- [29] J. P. Perdew, J. A. Chevary, S. H. Vosko, K. A. Jackson, M. R. Pederson, D. J. Singh, and C. Fiolhais, *Phys. Rev.*

- B*, **46**, 6671 (1992).
- [30] P. J. Feibelman, B. Hammer, J. K. Nørskov, F. Wagner, M. Scheffler, R. Stumpf, R. Watwe, and J. Dumesic, *J. Phys. Chem. B*, **105**, 4018 (2001).
- [31] G. Kresse, A. Gil, and P. Sautet, *Phys. Rev. B*, **68**, 073401 (2003).
- [32] T. E. Shubina and M. T. M. Koper, *Electrochim. Acta*, **47**, 3621 (2002).
- [33] M. T. M. Koper, T. E. Shubina, and R. A. van Santen, *J. Phys. Chem. B*, **106**, 686 (2002).
- [34] M. Lischka, C. Mosch, and A. Groß, *Electrochim. Acta*, **52**, 2219 (2007).
- [35] S. Sakong, C. Mosch, and A. Groß, *Phys. Chem. Chem. Phys.*, **9**, 2216–2225 (2007).
- [36] T. Hager, H. Rauscher, and R. J. Behm, *Surf. Sci.*, **558**, 181 (2004).
- [37] Y. Gohda and A. Groß, *J. Electroanal. Chem.*, **607**, 47 (2007).
- [38] Y. Gohda and A. Groß, *Surf. Sci.*, **601**, 3702–3706 (2007).
- [39] A. Roudgar and A. Groß, *Phys. Rev. B*, **67**, 033409 (2003).
- [40] A. Roudgar and A. Groß, *J. Electroanal. Chem.*, **548**, 121 (2003).
- [41] M. Ø. Pedersen, S. Helveg, A. V. Ruban, I. Stensgaard, E. Lægsgaard, J. K. Nørskov, and F. Besenbacher, *Surf. Sci.*, **426**, 395 (1999).
- [42] O. R. Inderwildi, S. J. Jenkins, and D. A. King, *Surf. Sci.*, **601**, L103–L108 (2007).
- [43] H. J. Kreuzer and S. H. Payne In *Computational Methods in Colloid and Interface Science*, M. Borowko, Ed.; Marcel Dekker, New York, 1999.
- [44] S. Müller, *J. Phys.: Cond. Matter*, **15**, R1429 (2003).
- [45] C. Stampfl, H. J. Kreuzer, S. H. Payne, H. Pfnür, and M. Scheffler, *Phys. Rev. Lett.*, **83**, 2993 (1999).
- [46] A. Bergbreiter, H. E. Hoster, S. Sakong, A. Groß, and R. J. Behm, *Phys. Chem. Chem. Phys.*, **9**, 5127–5132 (2007).
- [47] B. Sadigh, M. Asta, V. Ozoliņš, A. K. Schmid, N. C. Bartelt, A. A. Quong, and R. Q. Hwang, *Phys. Rev. Lett.*, **83**, 1379 (1999).